

Improving robustness of capacitive displacement measurements against electromagnetic disturbances in machine tool environments

Sebastian Böhl^{1,*}, Sascha Weikert², Konrad Wegener¹

¹*Institute of Machine Tools and Manufacturing (IWF), ETH Zürich,
Leonhardstrasse 21, 8092 Zurich, Switzerland*

²*Inspire AG, Technoparkstrasse 1, 8005 Zurich, Switzerland*

**E-mail address: boehl@iwf.mavt.ethz.ch*

Abstract

A systematic approach for determining electromagnetic disturbance effects on capacitive displacement transducers in machine tool environments is proposed. On the one hand these sensors offer high performance, on the other hand they are sensitive to electromagnetic disturbances. Hence, we recommend testing and characterising the sensor behaviour in machine tool environment in advance of the displacement measurement, in order to ensure the specified performance and an acceptable measurement uncertainty.

In a machine tool, perturbing sources, like motors and converters, can reduce the signal quality of capacitive sensors. Electromagnetic radiation and electrical conduction are potential coupling mechanisms between perturbing source and sensor. Depending on the specific type of sensor, disturbances can have severe impact on the measurement signal, when acting on the reference ground. To achieve high signal quality, the coupling of perturbing sources and sensor needs to be suppressed.

Basis of the presented approach is a cap test setup. A switchboard-like device is installed between target and reference ground, that allows individual connections to different potential perturbing sources. A suitable switching strategy between different connections enables separation of participating disturbance sources. Further, a configuration with potential minimal electromagnetic impact on the measurement device can be identified. The presented approach helps to enable capacitive displacement measurements with root mean square (RMS) noise values in machine tool environments that are close to RMS resolutions achieved during manufacturer calibration.

1 Introduction

Geometric testing of machine tools is an essential part of the machine tool acceptance process. Based on the ISO 230 series, testing procedures are defined to determine geometric accuracy of machine tools, which include component errors and position and orientation errors [1]. The testing of geometric accuracy of rotary axes is described in detail in ISO 230-7 [2]. Spindles are crucial components of machine tools, when chip removing processes are involved [3]. Depending on the type of spindle and the specific application purpose, different ranges of accuracy can be found in the market. In table 1 typical ranges of total radial error motion values for different types of spindles are indicated.

In order to verify specified tolerances, appropriate measurement techniques and devices are required. Non-contact capacitive displacement sensors can provide the necessary performance to carry out spindle measurements [4]. They are favourable, because of their capability of high resolution and large bandwidth. In dependence of their design and principle function, these sensors may show a high sensitivity to environmental disturbance effects.

Among others, electromagnetic disturbances can cause severe performance degradation, called electromagnetic interference (EMI). Prerequisite for the occurrence of disturbances are perturbing sources, that interact with the sensor, and available coupling paths between perturbing sources and sensor [5]. In case of geometric testing, the machine tool to be tested is given and cannot be modified regarding EMI. Therefore, the task is to prevent or to weaken coupling paths, like those based on electromagnetic radiation and electrical conduction.

The measurement device utilized for spindle measurements at the IWF is a Spindle Error Analyzer (SEA) from Lion Precision, which consists of five capacitive sensors (C7-C) and corresponding drivers (DMT20). The capacitive sensors have a sensitivity of 80 mV/ μm , a measuring range of $\pm 125 \mu\text{m}$ ($\pm 10 \text{ V}$), a bandwidth of 15 kHz and are operated in single-ended mode. The housings of the sensors are connected to the reference ground.

A National InstrumentsTM data acquisition unit (NI USB-6251) with 16 bit-resolution ($\approx 3.8 \text{ nm}$) is used to digitise the analogue signal, which is recorded in a measurement computer.

Experiments were carried out on the machine tool Präzoplan[®] [6], which is equipped with a Siemens SINUMERIK 840D SL CNC system. Linear drives and the spindle are controlled by SINAMICS S120 modules in standard configuration.

air bearing spindle	1	nm	<	Exc	<	100	nm
precision rolling bearings spindle	0.1	μm	<	Exc	<	1	μm
spindle for standard machine tool				Exc	>	1	μm

Table 1: Typical ranges of total radial error motion values (Exc) for spindles.

2 Problem Statement

The spindle error motion can be determined using the setup according to ISO 230-7 [2] shown in fig. 1a. The position and orientation of a test mandrel, typically made of steel, mounted in the spindle, are determined with five capacitive displacement sensors. A shaft grounding ring [7], connected to the reference ground of the measurement device, can be employed for target grounding in stand-still and during spindle rotation. This ring consists of conducting fibres, which are combined to a brush. To enhance conduction between brush and target, the mandrel is coated with a silver paint. The sensor fixture, also typically made of steel, is mounted directly on the machine tool table.

In a spindle measurement setup, the sensor is part of the structural loop between spindle and machine tool table. In addition, this mechanical closing implies electrical consequences [8]. The sensor system, consisting of the sensor driver, cable and sensor, is coupled to the electrical system of the machine tool. A highly simplified equivalent circuit diagram of the measurement setup for one sensor is shown in fig. 1b. Depending on setup and mounting aspects, different impedances may be introduced. Materials of components can have different specific ohmic material resistances or inductive properties, resulting in impedances Z_i . Furthermore, contact impedances Z_{ci} may be generated by the assembly of components due to contact resistances and to desired or undesired capacities. Disturbing voltages U_{Di} in combination with the impedances Z_i and Z_{ci} may mistune the measurement circuit. As consequence, the indicated value given by the evaluation unit might not only result from a mechanical change in gap width between sensor and

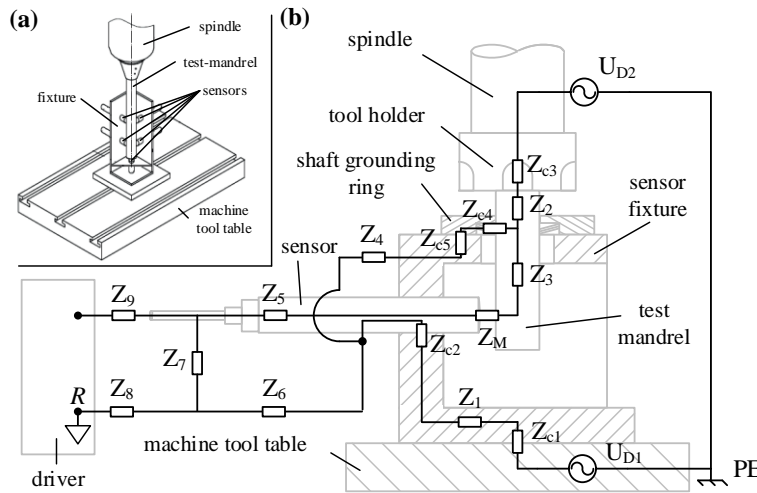


Figure 1: (a) Typical spindle measurement setup according to ISO 230-7 [2]. (b) Equivalent circuit for spindle measurement setup with reference ground R , protective earth ground PE , perturbing voltage sources U_{Di} , contact impedances Z_{ci} , material impedances Z_i and measurement impedance Z_M .

target, but also may contain components due to the disturbing voltages U_{Di} , which are generated in the machine tool. Potential sources for these disturbances are power electronics, drives and motors. Disturbances may encounter and travel as parasitic currents in the protective earth system (PE) of the machine tool [5].

The sensor target behaviour may be approximated, in the simplest way, by the impedance Z_M (fig. 1b), which consists of the measuring capacitance C_M , a loss resistance R_L and the resistance R_{iso} , representing the isolating behaviour of air in the gap between sensor electrode and target [9]. Changes in gap width $\Delta z(t)$ between sensor and target result in changes of the measuring capacitance C_M , which are detected in the downstream evaluation unit. The post processed value is transferred to the measurement computer as an indicated value $y(t)$. The impedance Z_M is a function of the voltage excitation frequency ω in the measuring circuit. The cable from the sensing device to the driver may introduce additional capacitive, inductive and resistive impedances. In order to detect mainly the desired changes of the capacitance C_M , due to mechanical variation in gap width, the different impedances of the measuring circuit need to be matched properly [9].

Assuming, that power electronics of the machine tool are the major perturbing sources and that disturbances couple into the measurement system by conduction, a galvanic separation of the measurement setup from the machine tool is regarded as a high potential method for weakening impacts of disturbances. This separation can be accomplished by using isolators. Beside the increase of resistance, such galvanic separations may introduce undesired capacities, which demand careful consideration. Compared to the measurement capacity these parasitic capacities shall be small [9].

The proposed testing method in this paper can be used to test the performance of the capacitive measurement system in different measurement setup configurations in machine tool environments. Especially, the effectiveness of the electrical decoupling of the measurement circuit from the machine tool can be tested.

Different potential coupling paths from perturbing sources into the sensor system and the measurement device are possible (see fig. 1b):

1. Disturbances may be transported via conduction from the spindle rotor via tool interface, tool holder, test mandrel and grounding ring into the grounding path.
2. Disturbances may travel, also via conduction, from the machine tool table via fixture and sensor housing into the grounding path.
3. Electromagnetic radiation generated by the machine tool, that acts on the sensor cables, couples into the shield and further into the reference ground.
4. Disturbances from the grid couple into the measurement system via the power supply either of the sensor drivers or the data acquisition unit. Disturbances may be generated in the sensor driving system, the data acquisition unit or the measurement computer equipment.
5. Disturbances, that are not caused by the machine tool, may couple into the measurement system via electromagnetic radiation (e.g. disturbances coming from various kinds of radio technology).

The mentioned coupling paths can be divided into three groups, namely those which are related to sources located in the machine tool (1-3), those which are

caused in the power supply of the measurement device or originate in the auxiliary equipment (4), and those which do not need a cable connection and are neither caused by the machine tool nor the measurement device (5).

The proposed method in this paper and the corresponding device mainly focus on the first two machine tool driven sources and related coupling mechanisms. Disturbances due to radiation acting on cables are weakened by cable shielding and adequate placing of cables, e.g. avoiding cable loops [5]. These are not further discussed. To reduce the impact of influences caused in the power supply of the measurement device a line filter can be applied or a battery as power supply can be used.

3 Testing Device

Nominally in a displacement measurement changes in gap width $\Delta z(t)$ between sensing electrode and target are evaluated. Due to the imperfect sensor behaviour and disturbing effects, as mentioned above, the output $y(t)$ of the sensor system, contains not only the mechanical target displacement, but also effects arising from disturbances $v(t)$. Therefore, the output $y(t)$ is a function of the target displacement $\Delta z(t)$ and disturbances $v(t)$. In order to analyse the influence of disturbances $v(t)$ independently of a mechanical displacement $\Delta z(t)$, the relative motion between target and sensor needs to be suppressed, $\Delta z(t) := 0$. Hence, the target and the sensor shall be mechanically coupled. This configuration is accomplished by a so-called cap test [10].

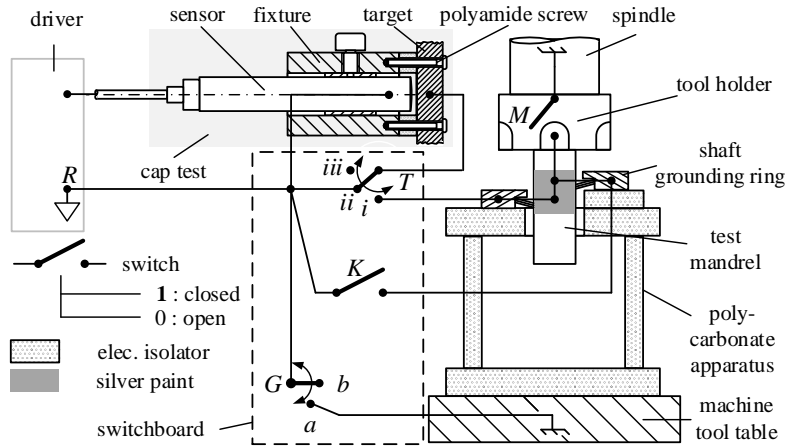
The novel test setup (fig. 2) is an extension of the regular cap test and is derived from the spindle measurement setup (fig. 1a):

Instead of measuring the displacement of a test mandrel, the sensors are mounted in an electrically conducting fixture and are capped with a steel target. A polycarbonate isolator is placed between sensor fixture and target. Polyamide screws are used for assembly. Thus, target and sensor housings are galvanically decoupled electrically and rigidly coupled mechanically.

The spindle measurement sensor fixture is replaced by a polycarbonate apparatus that is mounted on the machine tool table and carries the capped capacitive sensors and the shaft grounding ring. In this configuration the grounding ring is split in half. The segments are placed on two different height levels to avoid direct contact of the fibres of the two split rings. Despite the different height levels, the silver paint enables electrical conduction between the two ring segments.

In addition to the steel test mandrel, which is used for the geometric spindle testing, an electrically isolating mandrel is used. This mandrel consists of a cylinder, which is made of cotton fabric-base laminate with a phenolic resin matrix (EN PF CC 201, resofil). Analogous to the standard test mandrel, this cylinder is coated partly with a silver paint for electrical conduction from one half of the split grounding ring to the other. The resin cylinder can be used for assessing the effectiveness of electrical isolation of the measurement setup from the spindle.

All components of the test setup are nominally galvanically decoupled from each other. However, an electrical coupling between different components can be


Figure 2: Schematic of test device and switchboard.

Test Case	Switchboard Configuration								Description
	T1			T2		K	M		
	i	ii	iii	a	b				
1	<i>VI</i>	0	1	0	1	0	0	0	target coupled to machine tool table
2	<i>D1</i>	0	1	0	0	1	0	0	fully decoupled cap test
3	<i>D2</i>	1	0	0	0	1	1	1	target coupled to spindle
4	<i>D3</i>	1	0	0	0	1	1	0	decoupled spindle measurement setup
5	<i>D4</i>	0	1	0	1	0	0	0	target coupled to machine tool table

Table 2: Switching configurations for the test device discussed in this paper.

established via a switchboard-like device (fig. 2). The switches $T - \{i, ii, iii\}$ and K allow either a target configuration reflecting a floating ground, a direct coupling to reference ground R or a grounding path in which a rotating test mandrel is included. Instead, the switch $G - \{a, b\}$ in combination with switch M can be used to electrically interconnect either the spindle, the machine tool table or both with the reference ground. In table 2 test cases and corresponding settings on the switchboard are stated, which will be discussed in the following section.

4 Results

The following described experiments were carried out to enable the localisation and analysis of impacts of perturbing sources as well as assessing the effectiveness of isolating the measurement setup from the machine tool. The sampling frequency for the experiments discussed below is 250 kHz. In order to assess signal quality of the output $y(t)$, three different scalar measures are utilized, namely the root mean square value (*RMS*), the mean value \bar{y} and the standard deviation s (definitions according to [11]).

In this work the stated RMS resolution for a sensor in the calibration report is regarded as the lowest limit, that can be accomplished with the specific sensor at hand. The standard deviation proves to be a highly sensitive indicator in the presence of electromagnetic disturbances.

Test D1: In order to determine a lower limit for the RMS value, that is reachable under shop floor conditions with the proposed test setup, a sensor is tested in the machine tool working volume with machine tool power-off. The target is directly coupled to the reference ground (configuration 2 in tab. 2). For the recorded signal, which is symmetric and has zero-mean, a RMS value of 7.7 nm is determined. In this case, due to the zero-mean, the RMS value and the signal standard deviation are identical. The RMS value is close to the one stated in the manufacturer calibration report (RMS = 6.6 nm).

Test D2: The test device is set up in configuration 3 (tab. 2) on the machine tool, which is turned on. The target is galvanically decoupled from the machine tool table, but directly coupled to the spindle via the steel test mandrel and the shaft grounding ring segments. Therefore, effects of disturbances, travelling through the spindle into the measurement system, can be analysed. The test sequence is as follows, holding each state for $T = 9$ s: Starting with position control inactive (NC OFF) and then switching position control on (NC ON) for all linear axes and the spindle unit, the influence of the position control on the sensor behaviour is tested. Next, the spindle follows a speed profile with speed steps of 100 rpm between 100 rpm and 1'000 rpm and following steps of 2'000 rpm from 2'000 rpm up to 24'000 rpm. After finishing the speed profile, the spindle runs down, stops, remains in NC ON and finally the NC is turned off. The recorded signal and the calculated quality measures are shown in fig. 3 (red graphs). For the signal in operating mode NC OFF a standard deviation of 9.5 nm is calculated. Turning the machine in NC ON results in an increase of signal amplitude. The standard deviation remains between 105 nm and 135 nm until the NC is turned OFF again. The range of the shift of mean value over the whole sequence is $\Delta_{\text{mean,range}} \approx 60$ nm. Turning position control off results in the same low signal amplitudes, as observed in the beginning of the test sequence.

Test D3: The switching board configuration of *Test D2* is kept constant, but the steel test mandrel is replaced by the resofil cylinder (switch M open in fig. 2, configuration 4 in tab. 2). In doing so, the test setup is galvanically decoupled from the machine tool table as well as from the spindle. The same sequence as in *Test D2* is carried out. The measured signal is almost symmetric around the mean of each single tested operating condition (fig. 3, blue graphs). The shift of the mean stays in the range of $\Delta_{\text{mean,range}} \approx 12.7$ nm. The standard deviation is bounded for all tested operating conditions with $s < 10.3$ nm. This configuration shows high robustness against electromagnetic disturbances.

The mean values of the signal standard deviation for each operating condition averaged over eleven repetitions are shown in fig. 4. The error bars indicate the uncertainty of the mean values ($k = 2$), which includes uncertainty due to the resolution of the data acquisition unit and the standard deviation of the mean. The upper limit for the mean standard deviation, considering all tested operating conditions, is $\bar{s}_{\text{max}} = 10.5 \text{ nm} \pm 2.2 \text{ nm}$.

Test VI: In order to analyse the influence of the machine tool table, the test setup is operated in configuration 1 (tab. 2). The test sequence, described above, is carried out. Fig. 5 shows the voltage time record for the case with spindle speed of 100 rpm. The voltage $U(t)$, measured between reference ground and machine

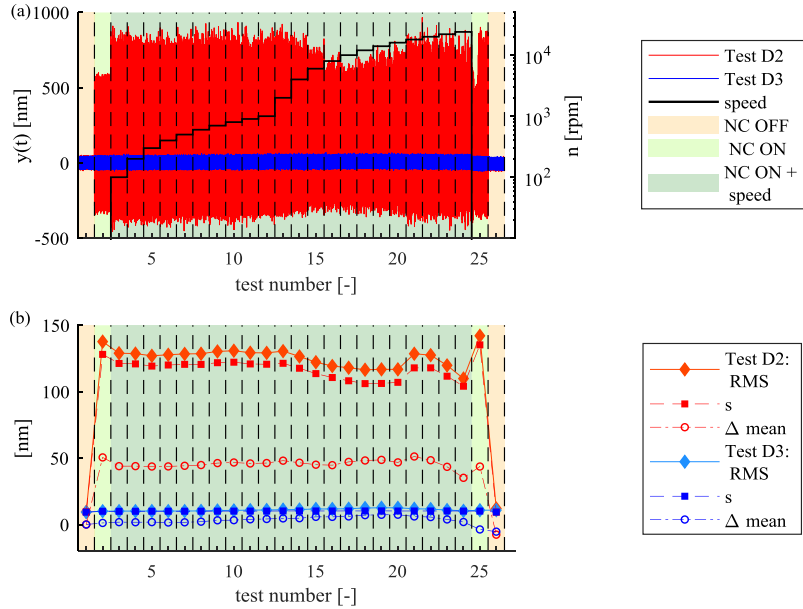


Figure 3: *Test D2*, target coupled to spindle; *Test D3*, target galvanically decoupled from machine tool: (a) time record for displacement output $y(t)$ at spindle speed n ; (b) scalar quality measures.

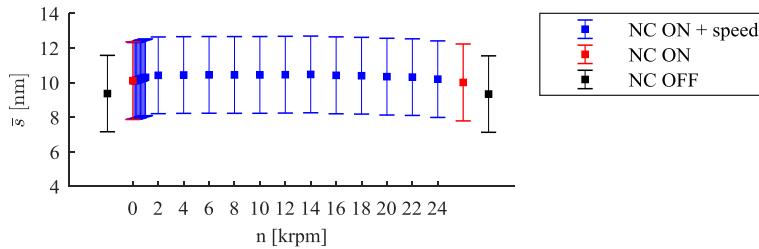


Figure 4: Standard deviation for repeated tests in configuration of *Test D3*.

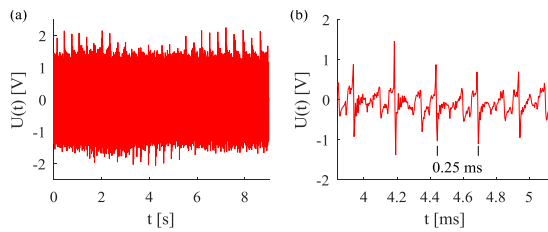


Figure 5: *Test VI*, target coupled to machine tool table, spindle speed 100 rpm: Time record in (a) full length and (b) zoom in on time scale.

tool table, shows a peak-to-peak value of approximately 4 V (fig. 5a). A more detailed look at the time record reveals a periodicity in the signal of 250 μs (fig. 5b), which corresponds to the current controller clock cycle time [12].

The switchboard configuration 5 (tab. 2) is tested in *Test D4*. This is the same configuration as for *Test V1*, only now the sensor displacement signal is recorded.

The data of *Test V1*, *Test D4* and *Test D3* are evaluated in frequency domain. A map is generated (fig. 6), which depicts the amplitude of the frequency components in relation to rotational spindle speed n . In the map of *Test V1* distinct vertical lines are apparent, especially accentuated at the frequencies 8 kHz and 12 kHz. The displacement data of *Test D4*, shows similar distinct lines. The target is coupled to the machine tool table in *Test V1* as well as in *Test D4*. The occurrence of the same distinct frequencies in both measurements, voltage and displacement, suggests, that disturbing voltages in the PE system of the machine tool influence the capacitive displacement measurement. Further, in case of galvanically decoupling the target from the machine tool (*Test D3*), the maximum amplitude can be reduced markedly compared to *Test D4*. This observation supports the hypothesis, that the impact of electromagnetic disturbances can be weakened by galvanic decoupling of the measurement setup from the machine tool.

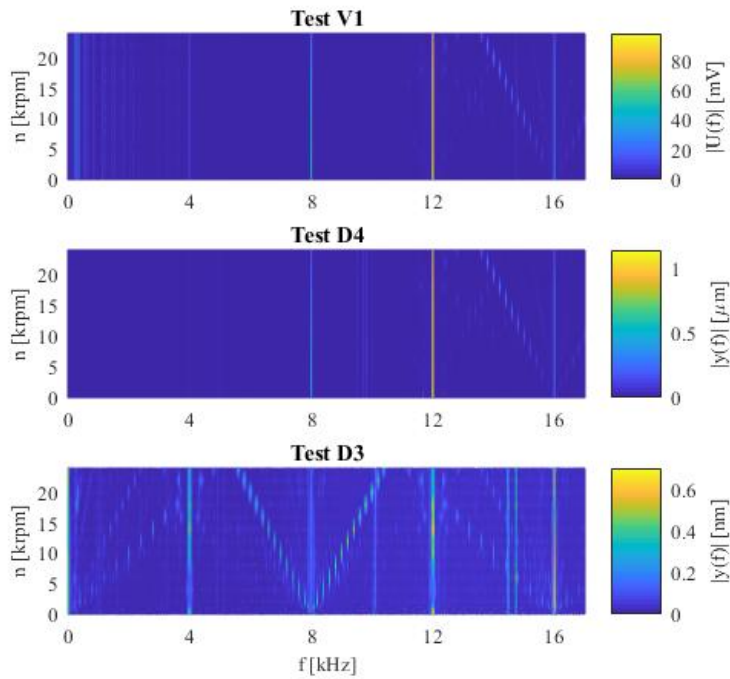


Figure 6: Frequency map: *Test V1*, target only coupled to machine tool table (voltage measurement); *Test D4*, target only coupled to machine tool table (displacement measurement); *Test D3*, decoupled spindle measurement setup (displacement measurement).

5 Discussion

The results of the experiments, discussed in the previous section, suggest, that the machine tool, especially the power electronics, generate significant disturbing effects for capacitive spindle measurements. On the one hand a shift in mean value of a signal is introduced, that might be interpreted erroneously as a mechanical shift. On the other hand, electromagnetic disturbances cause an increase of the signal standard deviation, which in turn increases the related standard uncertainty.

An effective measure to increase signal quality and to reduce disturbance influence is to electrically isolate the measurement setup from the machine tool. Adapting this knowledge to measurement setups for geometric spindle testing, means isolating the test mandrel from the spindle, isolating the sensor fixture from the machine tool table and ensuring that neither cables nor other components of the measurement setup electrically contact machine tool components. These measures weaken conductive coupling paths. Introduced capacities shall be small, compared to the measurement capacity, in order not to act counterproductively.

Minimizing the measuring gap increases the measurement capacitance and positively affects disturbance robustness. A carefully implemented measurement setup enables measurement signal qualities under shop floor conditions and in machine tool environments, that are close to signal qualities achieved under calibration conditions.

Acknowledgements We thank Wolfgang Knapp for his valuable comments and fruitful discussions.

References

- [1] ISO 230-1:2012(E) Test Code for Machine Tools – Part 1: Geometric accuracy of machines operating under no-load or quasi-static conditions.
- [2] ISO 230-7:2015(E) Test Code for Machine Tools – Part 7: Geometric accuracy of axes of rotation.
- [3] Abele E, Altintas Y, Brecher C (2010) Machine tool spindle units. *CIRP Ann. - Manuf. Technol.* 59: 781-802.
- [4] Marsh E R (2010) Precision Spindle Metrology. DEStech Publications, Lancaster.
- [5] Franz J (2013) EMV: Störungssicherer Aufbau elektronischer Schaltungen. Springer Vieweg, Wiesbaden.
- [6] Jaumann S (2012) PRÄZOPLAN®: Flächiges aerostatisches Führungssystem für spanende Werkzeugmaschinen. Dissertation, Eidgenössische Technische Hochschule Zürich.
- [7] Aegis® (2018) Bearing Protection Handbook. <https://www.est-aegis.com/literature.php>. Downloaded on 2019-02-11.
- [8] Sheridan T (1991) Know your machine tool. <http://www.lionprecision.com/tech-library/tech-notes/tech-pdfs/kynt.pdf>. Downloaded on 2018-12-05.
- [9] Rohrbach C (1967) Handbuch für elektrisches Messen mechanischer Grössen. VDI-Verlag, Düsseldorf.
- [10] ISO/DIS 230-3:2018(E) Test code for machine tools – Part 3: Determination of thermal effects.
- [11] Profos P (1981) Einführung in die Systemdynamik. Vieweg Teubner Verlag, Wiesbaden.
- [12] Siemens (2017) SINAMICS - Low Voltage Engineering Manual SINAMICS G130, G150, S120 chassis, S120 Cabinet Modules, S150 Supplement to Catalogs D 11 and D 21.3, version 6.5. https://cache.industry.siemens.com/dl/files/185/83180185/att_938805/v1/SINAMICS_Engineering_manual_V6.5_July_2017_external-e.pdf. Downloaded on 2018-11-29.